Human Molecular Genetics, 2003, Vol. 12, No. 5 **463–471**
DOI: 10.1093/hmg/ddg051

Usher syndrome type I G (USH1G) is caused by mutations in the gene encoding SANS, a protein that associates with the USH1C protein, harmonin

Dominique Weil[1,†], Aziz El-Amraoui[1,†], Saber Masmoudi[2,†], Mirna Mustapha[1], Yoshiaki Kikkawa[3], Sophie Lainé[1], Sedigheh Delmaghani[1], Avital Adato[1,4], Sellama Nadifi[5], Zeineb Ben Zina[6], Christian Hamel[7], Andreas Gal[8], Hammadi Ayadi[2], Hiromichi Yonekawa[3] and Christine Petit[1,*]

[1]Unité de Génétique des Déficits Sensoriels, CNRS URA1968, Institut Pasteur, 25 rue du Dr Roux, 75724 Paris cedex 15, France, [2]Laboratoire de Génétique Moléculaire Humaine, Faculté de Médecine, Sfax, Tunisia, [3]Department of Laboratory Animal Science, The Tokyo Metropolitan Institute of Medical Science (Rinshoken), Tokyo, Japan, [4]Department of Molecular Genetics and The Crown Human Genome Center, Weizmann Institute of Science, Rehovot, Israel, [5]Laboratoire de Génétique Humaine, Faculté de Médecine et de Pharmacie, Casablanca, Morocco, [6]Service d'Ophtalmologie, C.H.U. H. Bourguiba, Sfax, Tunisia, [7]INSERM U254, Laboratoire de Neurobiologie de l'Audition, Montpellier, France and [8]Institut für Humangenetik, Universitatsklinikum Hamburg-Eppendorf, Hamburg, Germany

Received December 6, 2002; Revised and Accepted January 7, 2003

Usher syndrome type I (USH1) is the most frequent cause of hereditary deaf–blindness in humans. Seven genetic loci (*USH1A-G*) have been implicated in this disease to date, and four of the corresponding genes have been identified: *USH1B*, *C*, *D* and *F*. We carried out fine mapping of *USH1G* (chromosome 17q24–25), restricting the location of this gene to an interval of 2.6 Mb and then screened genes present within this interval for mutations. The genes screened included the orthologue of the *Sans* gene, which is defective in the Jackson shaker deaf mutant and maps to the syntenic region in mice. In two consanguineous USH1G-affected families, we detected two different frameshift mutations in the *SANS* gene. Two brothers from a German family affected with USH1G were found to be compound heterozygotes for a frameshift and a missense mutation. These results demonstrate that *SANS* underlies USH1G. The SANS protein contains three ankyrin domains and a sterile alpha motif, and its C-terminal tripeptide presents a class I PDZ-binding motif. We showed, by means of co-transfection experiments, that SANS associates with harmonin, a PDZ domain-containing protein responsible for USH1C. In Jackson shaker mice the hair bundles, the mechanoreceptive structures of inner ear sensory cells, are disorganized. Based on the known interaction between USH1B (myosin VIIa), USH1C (harmonin) and USH1D (cadherin 23) proteins and the results obtained in this study, we suggest that a functional network formed by the USH1B, C, D and G proteins is responsible for the correct cohesion of the hair bundle.

INTRODUCTION

Usher syndrome (USH) is an autosomal recessive disease that affects both the inner ear and the retina. It is the most frequent cause of hereditary deaf-blindness, affecting 1 child in 25 000. Three clinical subtypes have been defined (1). USH type I (USH1), the most severe, involves severe to profound congenital sensorineural deafness, constant vestibular dysfunction and retinitis pigmentosa with prepubertal onset. USH2 differs from USH1 mainly in the deafness being less severe, the absence of vestibular dysfunction and the onset of retinitis pigmentosa after puberty. Finally, USH3 differs from USH1

*To whom correspondence should be addressed. Email: cpetit@pasteur.fr
†The authors wish it to be known that, in their opinion, the first three authors should be regarded as joint First Authors.

 © *Oxford University Press 2003; all rights reserved*

Downloaded from https://academic.oup.com/hmg/article/12/5/463/707029 by guest on 20 April 2024

and USH2 in the progressiveness of hearing loss and the occasional presence of vestibular dysfunction. USH1 is genetically heterogeneous. Seven loci responsible for this disease have been defined (*USH1A-G*) (2,3) and four of the corresponding genes have been identified: *USH1B*, *C*, *D* and *F*. *USH1B* encodes the actin-based motor protein myosin VIIa (4). *USH1C* encodes a PDZ domain-containing protein, harmonin (5,6). At least 10 isoforms of harmonin have been described. They may be classified into three subclasses referred to as harmonin a, b and c, and are collectively referred to as harmonin (6). Finally, mutations in the genes encoding two cadherin-related proteins, cadherin 23 and protocadherin 15, have been shown to cause USH1D (7,8) and USH1F (9,10), respectively.

Mutations have also been reported in three murine orthologs of the USH1 genes: *Myosin VIIa*, which is defective in shaker-1 (*sh1*) mutants (11); *Cadherin 23*, which is defective in waltzer (*v*) mutants (12), and *Protocadherin 15*, which is responsible for Ames waltzer (*av*) mutants (13). These mouse mutants are congenitally deaf and display vestibular dysfunction. In addition, the sensory cells of the inner ears of these mouse mutants display similar disorganization of the stereocilia comprising the hair bundle (12–14). We recently showed that myosin VIIA, harmonin and cadherin 23 interact in the developing inner ear sensory cells, ensuring the correct development of the hair bundle (15).

We studied a consanguineous Jordanian family affected by USH type 1 (JO-US1), and mapped the USH1G locus to an interval of 23 cM between markers D17S1350 and D17S1830 on chromosome 17q24–25 (3). In this study, we narrowed down the USH1G linkage interval, thanks to another USH1G-affected family, and identified *SANS*, the human orthologue of the gene defective in Jackson shaker (*js*) mutant mice (16), as the causative gene. We also showed, in co-transfection experiments, that SANS associated with harmonin, the protein underlying USH1C.

RESULTS AND DISCUSSION

Narrowing the limits of the USH1G interval

Eight members of a large family from Southern Tunisia (family MB) were recognized as suffering from profound congenital deafness. Vestibular dysfunction was assessed by caloric tests in patients MB15, 16, 18, 20, 29 and 30 (Fig. 1). Severe retinitis pigmentosa was assessed by funduscopy in all the affected children (see Materials and Methods). All the affected children were over the age of 16 years at the time of examination, with the exception of MB20, who was only 5 years old. The clinical features observed in this family qualify the disease as Usher syndrome type I.

We tested this family for co-segregation of the disease with any of the seven known *USH1* loci (*USH1A-G*), using polymorphic microsatellite markers (see Materials and Methods). Linkage was detected only with the markers of the USH1G interval, D17S1807 and D17S1603. We then tried to narrow down the USH1G interval, using markers located between D17S1350 and D17S1830, the two markers flanking the homozygosity region in the original USH1G family (Fig. 1). As affected individual MB20 was heterozygous for marker D17S1831, and the two affected individuals MB148 and MB152 were heterozygous for marker D17S1603, we were able to limit the USH1G interval to a 2.6 Mb region between these two markers (maximum LOD score 4.6, at $\theta = 0$ for markers D17S1807 and D17S1839).

SANS mutations cause USH1G

We first considered as candidate genes two genes located within the USH1G interval that corresponded to two cDNAs isolated from a subtracted cDNA library prepared from the vestibular sensory patches of the mouse inner ear (6). The first, the human giant larvae gene homologue (*LLGL2*) (GenBank accession number X87342) corresponded to a 3480 bp cDNA, extending over 19 kb, and comprised 23 exons (the 5′ end is missing from the Human Sequence Draft). Analysis of the sequences of these exons in USH1G-affected families (JO-US1 and MB) resulted in the detection of only silent polymorphisms. The other gene, solute carrier family 9 (sodium/hydrogen exchanger), isoform 3 regulatory factor 1 (*SLC9A3R1*) (GenBank accession number XM_046932), corresponded to a 1978 bp cDNA, extending over 21 kb and comprising 6 exons. No mutation of this gene was detected in either of the two affected families in analysing the sequences of the coding exons.

We previously reported that the locus involved in *js* mouse mutant, which presents deafness and vestibular dysfunction (17), mapped to a chromosomal region syntenic to the human *USH1G* region (3). Although the *USH1G* interval identified here was much smaller, it nonetheless still matched with the *js* locus. As the *Sans* gene was recently shown to be mutated in *js* mice (16), we considered the human orthologue *SANS* (GenBank accession number AK091243) as a candidate gene responsible for USH1G. *SANS* is located between markers D17S1807 and D17S1839. The cDNA for this gene is 3559 bp long. Comparison with human genome sequences (GenBank accession number AC068874) revealed that *SANS* encompasses 7.2 kb and comprises three exons, two of which are coding. The 1380 bp open reading frame (ORF) is predicted to encode a 460 amino acid (aa) protein. The translation initiation site was identified at position 184 on the basis of the presence of a Kozak consensus sequence (gcgccATGaacga) preceded by an in-frame stop codon, 170 bp upstream. The human and mouse ORFs display 90% nucleotide sequence identity, and the two predicted protein sequences are 96% identical. Sequence analysis of the encoded protein showed this protein to contain three ankyrin-like domains (18) at the N-terminal end (aa 31–63, 64–96 and 97–129), a central region (aa 130–385), and a SAM (sterile alpha motif) domain (19) (aa 384–446; Fig. 2) and a PDZ-binding motif at the C-terminal end. This protein was therefore named SANS for *s*caffold protein containing *an*kyrin repeats and *S*AM domain. Ankyrin domains are involved in protein–protein interactions (18). SAM domains, originally identified in yeast (19), are present in several proteins involved in the regulation of a number of developmental processes (e.g. protein kinase receptors, cytoplasmic scaffolding proteins, transcription factors). These domains, which are thought to be involved in protein–protein interactions, may undergo homo- or heterodimerization with other SAM domains (20,21).

Downloaded from https://academic.oup.com/hmg/article/12/5/463/707029 by guest on 20 April 2024

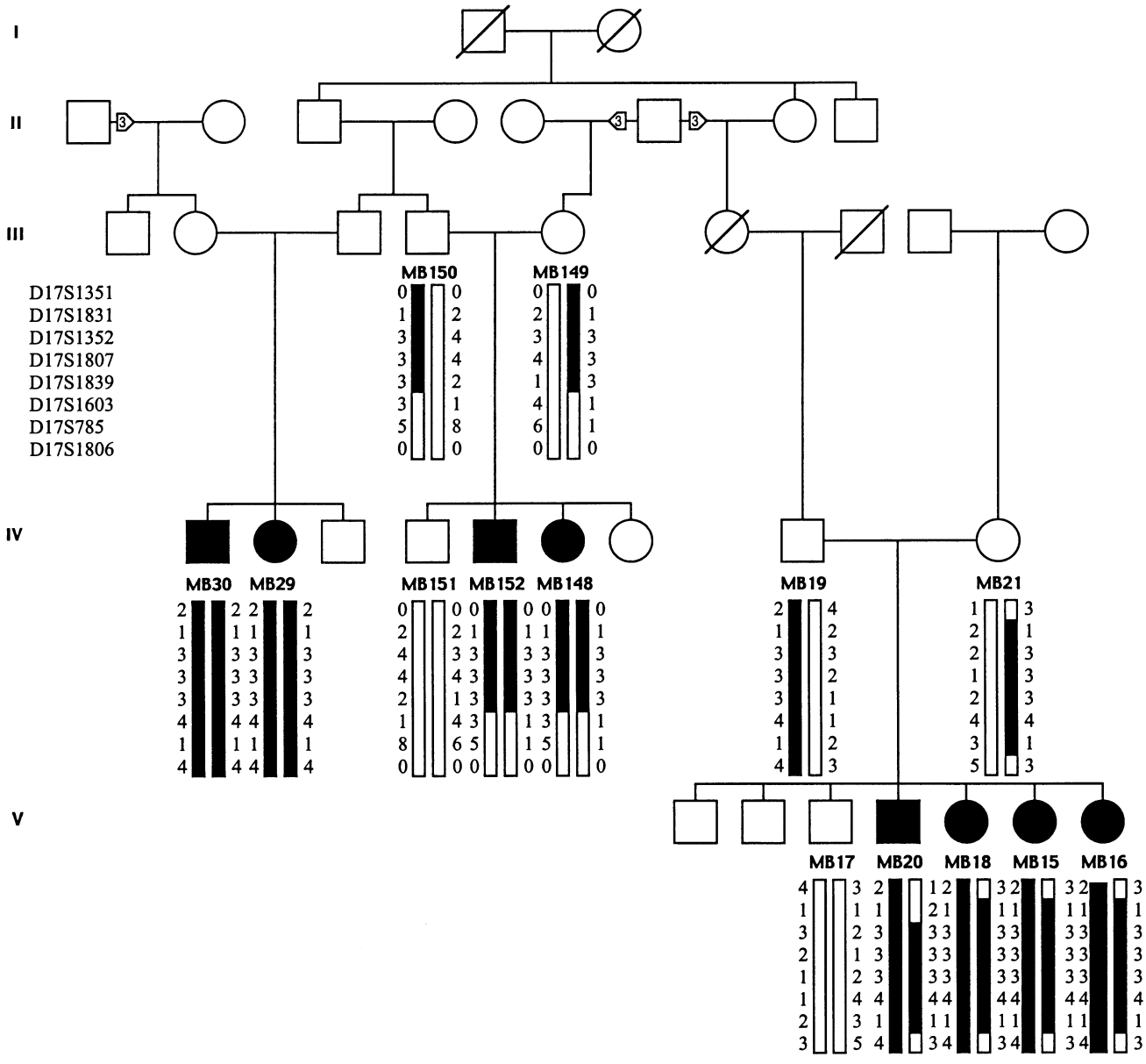

Figure 1. Segregation of eight polymorphic microsatellite markers from the 17q24–25 chromosomal region in family MB. Solid symbols represent affected individuals. Analysis of the haplotypes of individuals MB20, MB152 and MB148 defined the USH1G minimal interval as the 2.6 Mb region between D17S1831 and D17S1603.

We designed primers (Table 1) to amplify and sequence the two coding exons and the flanking intronic regions. In the three affected members of family JO-US1 (3), a 20 bp deletion (829–848del) was detected in exon 2, in the homozygous state (Figs 2 and 3A). The deletion was also found in a heterozygous state in both parents of these individuals and in their three unaffected siblings. This frameshift deletion is predicted to lead to the production of a truncated protein, only 326 aa long (i.e. without the SAM domain), the last 70 residues of which are not in-frame. In the eight affected members of family MB, the insertion of a single base (393insG) was detected in exon 2, in the homozygous state (Figs 2 and 3B). The mutation was present in the heterozygous state in the parents, and was absent from the unaffected individuals MB17 and MB151. This frameshift mutation is predicted to lead to the production of a 133 aa protein, in which only the three ankyrin repeats could possibly be preserved.

We then analysed 39 sporadic and familial USH1 cases from Germany, France, Israel, Iran and Morocco. In 19 of these cases, no mutation had been detected in the gene encoding myosin VIIA (responsible for USH1B) or in the gene encoding harmonin (USH1C). In six other patients, no linkage had been found to the USH1B locus. Two brothers (patients 54 and 55) of German origin were found to be compound heterozygotes for *SANS* mutations. One allele carried a C to T transition (142C > T) in exon 1, which was predicted to lead to a L48P

Downloaded from https://academic.oup.com/hmg/article/12/5/463/707029 by guest on 20 April 2024

Figure 2. Predicted amino-acid sequence of the human SANS protein. The three predicted ankyrin domains are indicated in red and blue (aa positions 31–63, 64–96 and 97–129) and the SAM domain (aa positions 384–446) in green. (**A**) Site of the deletion found in the family JO-US1. (**B**) Site of the insertion found in family MB. (**C**) Site of the deletion found in patient 54, the substitution resulting from the 142C > T transition in patient 54 (L48P) is highlighted in yellow.

Table 1. Sequences of primers used for the amplification and sequencing of the two Sans coding exons. Primers a and m were used for amplification and sequencing, and primers 2F and 2R for sequencing only

Exon 1a	5′-GGGTGAGCGTTTCAGATGTCTTG-3′
Exon 1m	5′-GGCAGCTCAGAGGAGTGGTGGA-3′
Exon 2a	5′-CTGTGACAGTGGGGAAGCTCCC-3′
Exon 2m	5′-CCTGAATAGGCAGATCTGTACCCCC-3′
Exon 2F	5′-TCTCCGAGGATGGGCGCAAG-3′
Exon 2R	5′-GAGGAACATGTCCCGGAGCGG-3′

substitution, whereas a dinucleotide deletion in exon 2 (186–187delCA) of the second allele (Figs 2 and 3C1 and C2) was predicted to lead to the production of a truncated protein 132 aa long, the last 70 residues of which were predicted not to be in-frame. Each mutation was found in a heterozygous state in one parent, the mother carrying the missense mutation and the father the frameshift deletion. The L48P aa substitution occurs in the first ankyrin domain of the SANS protein, at a position at which none of the 442 ankyrin domain sequences analysed has a proline (leucine, valine or isoleucine is present at this position in 75% of the sequences; http://smart.embl-heidelberg.de) and is therefore expected to be deleterious. None of the detected mutations was found in 80 control individuals. These results identify *SANS* as the gene responsible for USH1G.

We previously suggested (3) that USH1G and two genetic forms of dominant late-onset hearing loss, DFNA20 (22) and DFNA26 (23), might be allelic disorders because they have overlapping linkage intervals. As *SANS* is located outside the interval defined for these two forms of isolated deafness, it is very unlikely that *SANS* is also involved in either DFNA20 or DFNA26.

Sans interacts with harmonin

As ankyrin repeat-containing proteins have been reported to be linked to the cytoskeleton (18), we explored the possible association of Sans with the cytoskeleton. A full-length *Sans* cDNA encoding a myc-tagged Sans protein was generated. In transfected HeLa cells, immunolabelling for Sans gave a uniform pattern of punctate staining throughout the body of the cell (Fig. 4A). Double immunolabelling with rhodamine-phalloidin or with antibodies directed against α-tubulin, cytokeratin 18 or vimentin, or a pan-cytokeratin antibody showed that Sans was not associated with actin microfilaments, microtubules or intermediate filaments (Fig. 4A and data not shown).

A database search for sequences similar to that of Sans revealed that the most similar protein was Harp, which was reported as harmonin interacting protein (GenBank accession number AF524030). The Harp and Sans proteins were predicted to display 41% sequence identity and 65% sequence similarity (the ankyrin and SAM domains of the two proteins were predicted to be 72 and 51% identical, respectively). The two proteins differed principally in the central region, which was more divergent (26% identity) than the terminal regions. The last three aa of the human and murine Sans proteins (TEL) and of the murine Harp (TSL) protein match the class-I PDZ-interacting consensus sequence (S/T-X-Φ, where X is any aa and Φ is hydrophobic (24). We therefore carried out co-transfection experiments in HeLa cells to determine whether any of the three harmonin subclasses (a, b and c) (6) interacted with Sans. In cells producing both harmonin and Sans, harmonin b was associated either with punctate structures (Fig. 4B–D) or with long, curved filaments (Fig. 4E–G), throughout the cytoplasm, displaying perfect co-localization with Sans (Fig. 4D). This co-localization appeared to be specific because no such pattern

Downloaded from https://academic.oup.com/hmg/article/12/5/463/707029 by guest on 20 April 2024

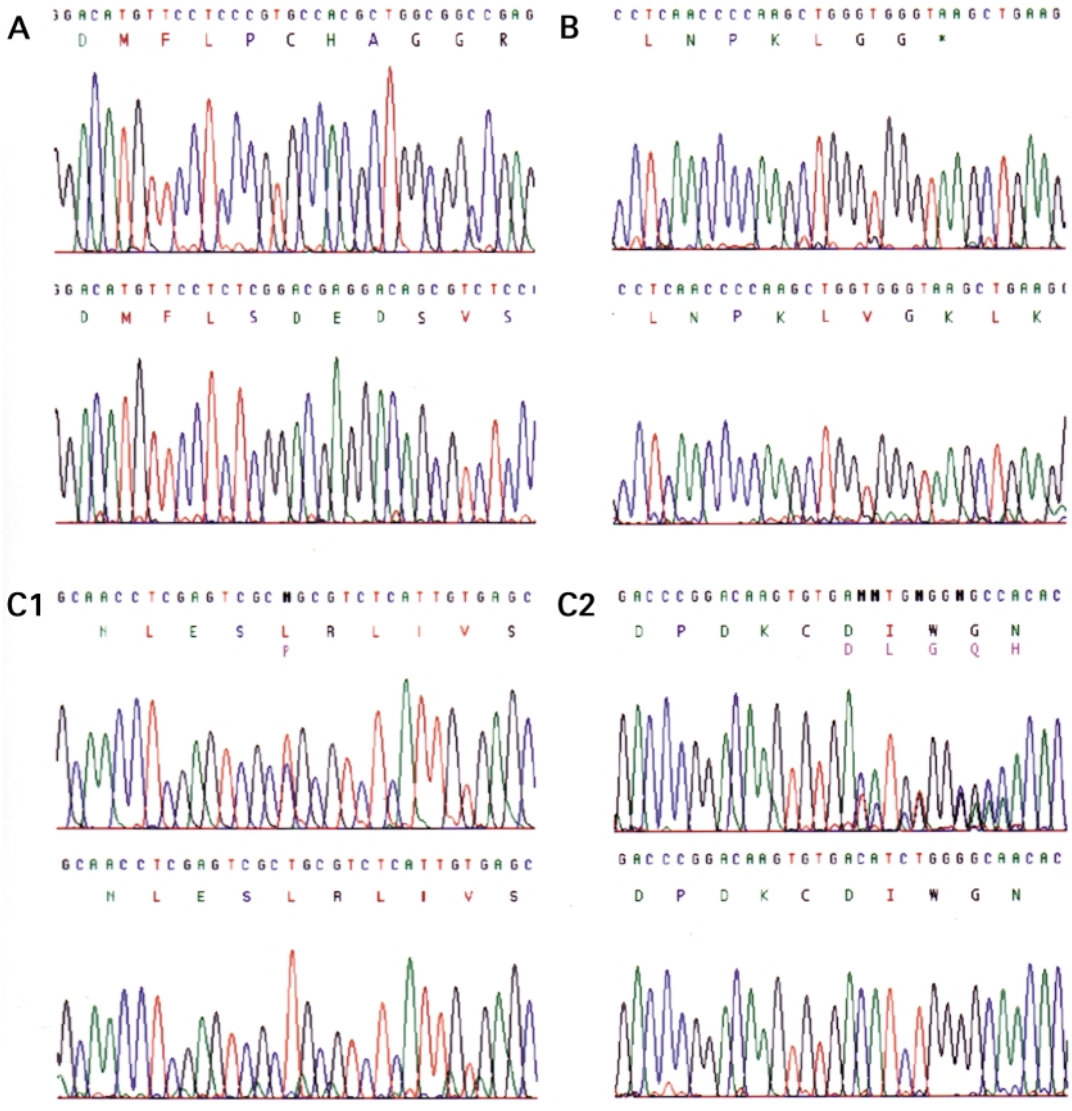

Figure 3. Four mutations in the *SANS* gene in three USH1G patients. The mutated sequence is shown in the upper panel and below the corresponding wild-type sequence. The deduced amino-acid sequence is indicated below the DNA sequence. (**A**) Affected individual in family JO-US1, homozygous for a 20-nucleotide deletion in exon 2. (**B**) Affected individual in family MB, homozygous for a one-base insertion in exon 2 (393insG). (**C**) Affected individual 54. (1) Heterozygous substitution in exon 1 (C182T). (2) Heterozygous deletion in exon 2 (186–187delCA).

was observed on co-transfection with constructs encoding Sans and either green fluorescent protein (GFP)-tagged Rab4 or GFP-tagged vezatin (Fig. 4J and data not shown). We recently showed that harmonin b, the longest harmonin isoform, directly binds actin filaments, inducing the formation of large actin bundles, whereas harmonin a and harmonin c do not (15). In co-transfected cells producing both Sans and harmonin b, the presence of harmonin b modified the distribution of Sans: the punctate Sans-labelled structures were replaced by longer filaments that were also labelled with rhodamine-phalloidin (Fig. 4E–G). This suggests that harmonin b may connect Sans to actin filaments. Moreover, co-transfection experiments with harmonin a and c revealed that the distribution of Sans was identical to that of these harmonin isoforms (Fig. 4H, and data not shown). To identify the harmonin PDZ domain involved in this interaction, we co-transfected cells with a construct encoding Sans and with a cDNA encoding either the PDZ1, PDZ2 or PDZ3 domain (see Materials and Methods). Sans was entirely co-localized with the PDZ1 domain (Fig. 4I) and partially co-localized with the PDZ2 domain, whereas no co-localization was observed with the PDZ3 domain (not shown). These results suggest that Sans interacts with harmonin by binding to the first PDZ domain of harmonin. Consistent with these results, Harp has also been reported to interact with the harmonin PDZ1 domain (GenBank accession number AF524030).

We then used RT–PCR to investigate the expression of *Sans*, *Harp* and the harmonin gene, in the inner ear, eye and kidney (Fig. 5). Interestingly, whereas both the genes associated with USH1 were expressed in the inner ear and eye, no *Harp* expression was detected in these sensory organs. In contrast, in the kidney, we observed transcription of the *Harp* and

Downloaded from https://academic.oup.com/hmg/article/12/5/463/707029 by guest on 20 April 2024

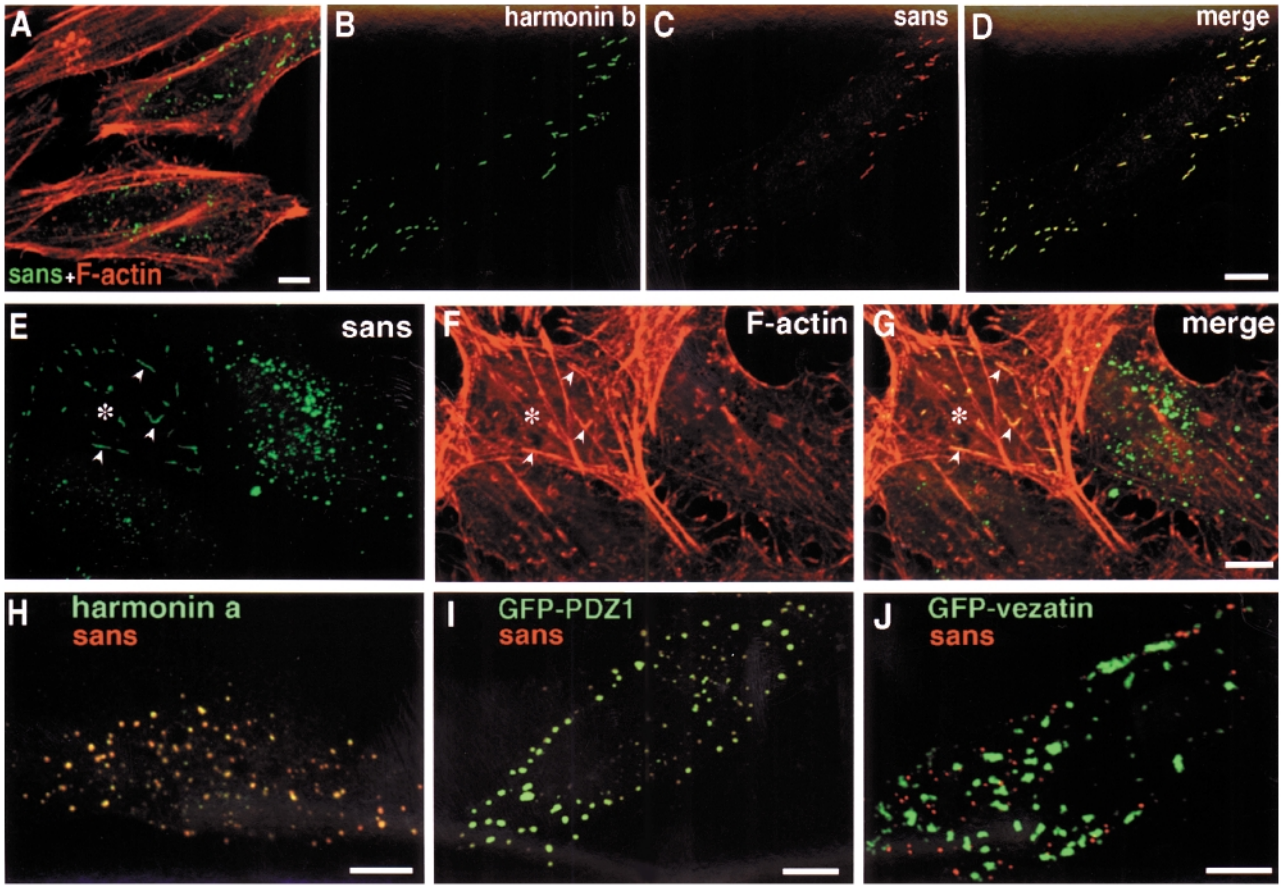

Figure 4. (**A**) Sans in transfected HeLa cells. Sans (green) is distributed throughout the cytoplasm. No association with actin filament-labelled structures (red) is observed. (**B**–**D**) Sans associates with harmonin b. In HeLa cells producing harmonin b (B) and Sans (C), the two proteins show identical distributions throughout the cell (D). (**E**–**G**) Harmonin b connects Sans to F-actin. The presence of harmonin b clearly changes the distribution of Sans-labelled structures (green). The cell on the right produces Sans only whereas the cell on the left (asterisk) produces both Sans and harmonin b. In the cell on the right, Sans displays a punctate distribution and no co-localization with actin filaments (red). In contrast, in cells producing both Sans and harmonin b (asterisk), the punctate or the long filamentous structures labelled show the same distribution as actin (arrowheads). (**H**–**J**) Sans associates with harmonin a (H) and the GFP-tagged PDZ1 domain of harmonin (I), but not with GFP-tagged vezatin (J). In co-transfected HeLa cells, Sans immunolabelling (red) displayed a distribution identical to that of harmonin a (H) and GFP-tagged PDZ1 (I), throughout the cell cytoplasm (yellow). In contrast, no co-localization of Sans (red) with GFP-vezatin (green in J) was observed. Bars: 10 μm.

harmonin genes but detected no *Sans* transcripts (Fig. 5). The differential tissue expression of *Sans* and *Harp* suggests that the central region of Sans, which diverges from that of Harp, plays a specific role in the inner ear and the eye.

Sans, which is produced in the sensory hair cells (16), may be connected to the actin cytoskeleton via its interaction with harmonin b, an isoform largely restricted to the inner ear (6). From our previous (15) and present studies, the following picture emerges: Sans interacts with harmonin, a scaffolding protein that itself binds to myosin VIIa and cadherin 23; the harmonin b isoform also binds actin filaments (see Fig. 6). Harmonin, myosin VIIa and cadherin 23 are detected in the growing hair bundles of the inner ear sensory cells (15,24). Harmonin b may anchor cadherin 23-containing interstereociliar links to the actin filament cores of growing stereocilia (Fig. 6) (15).

The results of this study suggest that Sans is involved in the functional network formed by harmonin, cadherin 23 and myosin VIIa that is required for cohesion of the growing hair bundle. Consistently, the *js* (Sans) mouse mutant displays disorganization of the hair bundle (26) similar to that observed in *sh1* (myosin VIIa) (14) and *v* (cadherin 23) (12) mouse mutants. The possible involvement in the network of protocadherin 15 (USH1F) and of the proteins underlying the other forms of USH1 remains to be determined.

MATERIALS AND METHODS

Patients

Informed consent was obtained from adult subjects and from the parents of patients below the age of consent.

Clinical studies

Hearing loss was quantified by pure-tone audiometry with aerial and bone conduction at 250, 500, 1000, 2000, 4000 and

Downloaded from https://academic.oup.com/hmg/article/12/5/463/707029 by guest on 20 April 2024

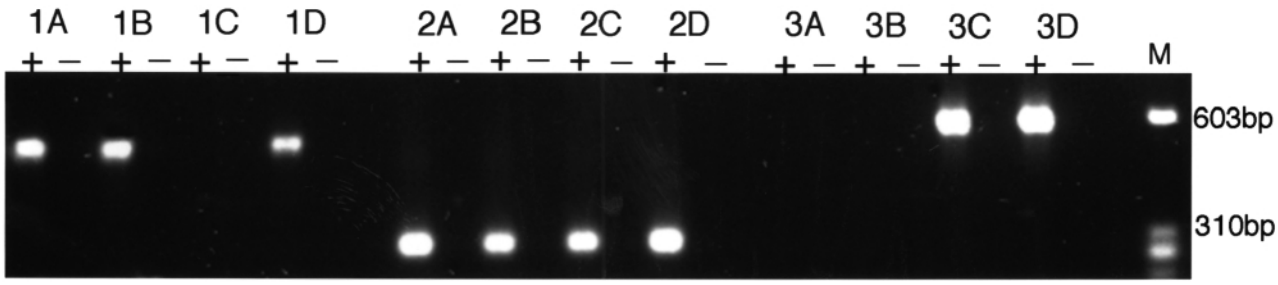

Figure 5. RT–PCR analysis of *Sans*, *harmonin* and *Harp* expression in various tissues: *harmonin* (**2A**–**D**) is expressed in the vestibule (A), the eye (B), the kidney (C) and the small intestine (D); *Sans* (**1A**–**D**) is expressed in the vestibule (A), the eye (B), and the small intestine (D); and Harp (**3A**–**D**) is expressed in the kidney (C) and the small intestine (D). M: DNA marker.

8000 Hz (Beltone 2000 clinical audiometer), in every individual over the age of 5 years. Air conduction pure-tone average (ACPTA) threshold in the conversational frequencies (0.5,1 and 2 kHz) was calculated for each ear, and hearing loss was classified as mild ($20 \leq$ ACPTA ≤ 40 dB), moderate ($40 <$ ACPTA ≤ 70 dB), severe ($70 <$ ACPTA ≤ 90 dB), or profound (ACPTA > 90 dB). In younger children, auditory function was explored by recording audiometric brain response (ABR). Vestibular dysfunction was assessed by caloric test. Retinitis pigmentosa was diagnosed by funduscopy and functional impairment was assessed on an electroretinogram (ERG).

Genotyping

Fluorescent polymorphic microsatellite markers were used. PCR products were analysed by electrophoresis in a 6% polyacrylamide gel. The markers used for the linkage analysis of the MB family with the known USH1 loci were: D14S250, D14S1006, D14S985, D14S1051, D14S292, D14S272, D14S1010, D14S260 for USH1A; D11S527, D11S906, D11S4186 for USH1B; D11S902, D11S4099, D11S4096 for USH1C; D10S206, D10S1786, D10S532 for USH1D; D21S1884, D21S1257, D21S265 for USH1E; D10S189, D10S1684, D10S596 for USH1F and D17S1831, D17S1807, D17S1603 for USH1G (sequences available at ftp://ftp.genethon.fr/pub/Gmap/Nature-1995/data).

Linkage analysis

LOD scores were calculated using the FASTLINK version of the Linkage Program Package (27). The defect was assumed to be inherited, recessive and fully penetrant. The disease allele frequency was estimated at 10^{-3}. The allele frequencies for the polymorphic markers, and meiotic recombination frequencies in males and females, were assumed to be equal.

Sequence analysis

Nucleotide and protein sequence comparisons were carried out with EMBOSS (www.uk.embnet.org/Software/EMBOSS/). The presence of the various domains was assessed with Interpro (www.ebi.ac.uk/interpro/).

Mutation screening

We established the exon/intron structure of the gene by comparing the human cDNA sequences (GenBank accession number AK091243) with the draft human genome sequence (http://genome.ucsc.edu, UCSC, Human Genome Project Working Draft, December 22, 2001). We designed primers for the amplification and sequencing of the two coding exons and their flanking splice sites (see Table 1). These exons were amplified by PCR and sequenced as previously described (6).

RT–PCR

Reverse transcription was performed with 1 μg of total RNA, an oligo (dT) primer and SuperScript II RNase H^- Reverse Transcriptase (Invitrogen). The full-length cDNA was reconstituted from brain mRNA. One-tenth of the reaction product was amplified by PCR in a total volume of 50 μl, using forward primer 5′-ATGAACGACCAGTACCACCGGG-3′ and reverse primer 5′-AAACACCCCAGCTGTGATTCCTGTG-3′. RT–PCR analysis was used to assess gene expression in the inner ear, eye, kidney and small intestine of mice on postnatal day 2 (P2), with the following primers: Sans forward, 5′-CCTACCATGGCAACCTGGAGTC-3′; Sans reverse, 5′-AGCTTCTTCTGGATCTTGGCC-3′; harmonin forward, 5′-GAAGGCTGCCGAGGAGAATGAG-3′; harmonin reverse, 5′-CTGCGATCTGCTCTGGCGAGAA-3′; harp forward, 5′-ACACCCACTCTCCTGGCAGCCTAC-3′, harp reverse, 5′-CAGGCCTCTGCCCACTTCTTC-3′. The reactions were carried out according to a standard protocol, using 30 cycles and the Expand High-Fidelity PCR system (Roche).

Cell lines and immunofluorescence analysis

HeLa cell lines were cultured in Dulbecco's modified Eagle medium (DMEM) supplemented with 10% fetal calf serum (FCS). Cells were transiently transfected, using Effectene (Qiagen). Immunohistofluorescence analysis was carried out on fixed cells, as previously described (28). Briefly, HeLa cells were incubated for 15 min with 50 mM NH_4Cl in phosphate-buffered saline (PBS), then washed in 0.01% saponin in PBS. The cells were incubated for 1 h in 10% goat serum in PBS, and then with the anti-myc antibody for 1 h at room temperature (RT), followed by the secondary antibody, also for 1 h at RT. Slides were examined under a conventional epifluorescence

Downloaded from https://academic.oup.com/hmg/article/12/5/463/707029 by guest on 20 April 2024

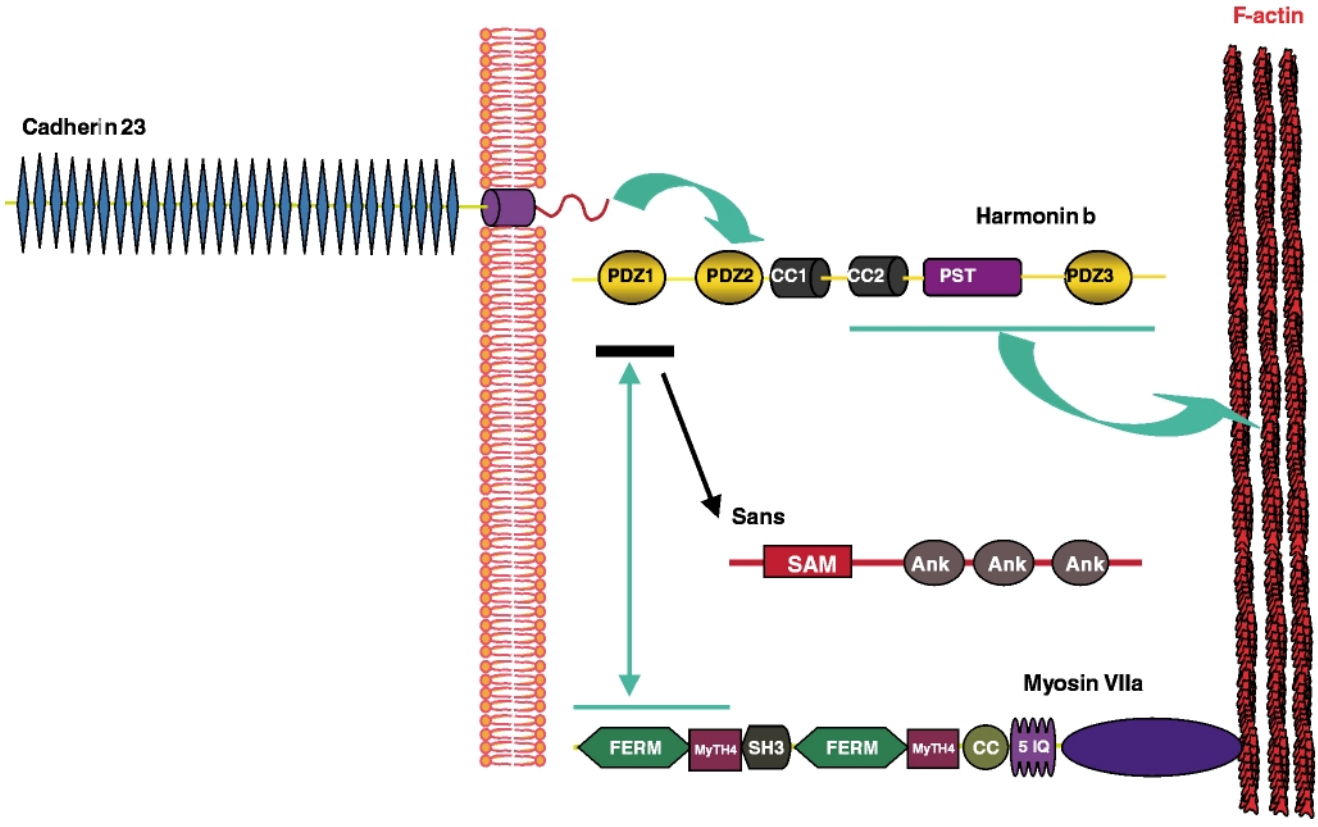

Figure 6. Schematic diagram illustrating the possible interactions of harmonin b with myosin VIIa, cadherin 23, Sans and F-actin (25). The cytodomain of cadherin 23 (USH1D), which is located in the membrane of stereocilia, interacts with harmonin b (USH1C) via the PDZ2 domain. The actin-based motor protein, myosin VIIa (USH1B), also binds to harmonin b, via the PDZ1 domain. Harmonin b also binds actin filaments via its C-terminal region, and is therefore thought to connect cadherin 23 stereocilia laterally to the stereocilia microfilaments. Sans (USH1G) binds harmonin b, via the PDZ1 domain. PDZ, post synaptic density, disc large, zonula occludens domains; CC, coiled-coil domain; PST, proline, serine, threonine (PST)-rich region; Ank, ankyrin repeats; SAM, sterile alpha motif; FERM, 4.1, ezrin, radixin, moesin; MyTH4, myosin tail homology 4; SH3, src homology-3; IQ, isoleucine-glutamine motifs; EC, extracellular cadherin repeats.

microscope (Leica) or a laser scanning confocal microscope, LSM-540 (Zeiss).

The following mouse monoclonal antibodies were used: anti-Myc (clone 9E10) (Santa Cruz); anti-α-tubulin; and anti-pan cytokeratin (Sigma). Rhodamine-phalloidin (Sigma) staining was used to visualize actin filaments.

The full-length mouse cDNAs encoding harmonin isoforms a, b, and c subcloned into pcDNA (Invitrogen) have been described elsewhere (15). cDNAs encoding truncated forms of harmonin—PDZ1 (aa: 72–88), PDZ2 (189–307) and PDZ3 (738–849)—were inserted into the pECFP vector (Clontech). The full-length mouse cDNA encoding Sans was inserted into the myc-tagged pCMV vector (Stratagene).

ACKNOWLEDGEMENTS

We thank Marino Zerial (Dresden, Germany) for the gift of the GFP-Rab4 plasmid, J. Levilliers, J.-P. Hardelin, M. Leibovici, E. Verpy and S. Cure for critical reading of this manuscript, S. Nouaille for help with genotyping and S. Chardenoux for drawing the figures. We also thank M. Leibovici and E. Verpy for supplying us with mouse tissue RNAs. This work was supported by grants from Fondation pour la Recherche Médicale (ARS2000), INSERM/CNCPRST Santé Publique, Fondation Srittmatter (Retina France), A. and M. Suchert Forschung contra Blindheit-Initiativ Usher syndrome and the European Community (QLG2-CT-1999-00988).

REFERENCES

1. Otterstedde, C.R., Spandau, U., Blankenagel, A., Kimberling, W.J. and Reisser, C. (2001) A new clinical classification for Usher's syndrome based on a new subtype of Usher's syndrome type I. *Laryngoscope*, **111**, 84–86.
2. Petit, C. (2001) Usher syndrome: from genetics to pathogenesis. *A. Rev. Genomics Hum. Genet.*, **2**, 271–297.
3. Mustapha, M., Chouery, E., Torchard-Pagnez, D., Nouaille, S., Khrais, A., Sayegh, F.N., Megarbane, A., Loiselet, J., Lathrop, M., Petit, C. *et al.* (2002) A novel locus for Usher syndrome type I, USH1G, maps to chromosome 17q24-25. *Hum. Genet.*, **110**, 348–350.
4. Weil, D., Blanchard, S., Kaplan, J., Guilford, P., Gibson, F., Walsh, J., Mburu, P., Varela, A., Levilliers, J., Weston, M.D. *et al.* (1995) Defective myosin VIIA gene responsible for Usher syndrome type 1B. *Nature*, **374**, 60–61.
5. Bitner-Glindzicz, M., Lindley, K.J., Rutland, P., Blaydon, D., Smith, V.V., Milla, P.J., Hussain, K., Furth-Lavi, J., Cosgrove, K.E., Shepherd, R.M. *et al.* (2000) A recessive contiguous gene deletion causing infantile hyperinsulinism, enteropathy and deafness identifies the Usher type 1C gene. *Nat. Genet.*, **26**, 56–60.

Downloaded from https://academic.oup.com/hmg/article/12/5/463/707029 by guest on 20 April 2024

6. Verpy, E., Leibovici, M., Zwaenepoel, I., Liu, X.-Z., Gal, A., Salem, N., Mansour, A., Blanchard, S., Kobayashi, I., Keats, B.J.B. *et al.* (2000) A defect in harmonin, a PDZ domain-containing protein expressed in the inner ear sensory hair cells, underlies Usher syndrome type 1C. *Nat. Genet.*, **26**, 51–55.
7. Bolz, H., von Brederlow, B., Ramirez, A., Bryda, E.C., Kutsche, K., Nothwang, H.G., Seeliger, M., Salcedo Cabrera, M.d.C., Vila, M.C. *et al.* (2001) Mutations of *CDH23*, encoding a new member of the cadherin gene family, causes Usher syndrome type 1D. *Nat. Genet.*, **27**, 108–112.
8. Bork, J.M., Peters, L.M., Riazuddin, S., Bernstein, S.L., Ahmed, Z.M., Ness, S.L., Polomeno, R., Ramesh, A., Schloss, M., Srisailpathy, C.R.S. *et al.* (2001) Usher syndrome 1D and non-syndromic autosomal recessive deafness DFNB12 are caused by allelic mutations of the novel cadherin-like gene *CDH23*. *Am. J. Hum. Genet.*, **68**, 26–37.
9. Ahmed, Z.M., Riazuddin, S., Bernstein, S.L., Ahmed, Z., Khan, S., Griffith, A.J., Morell, R.J., Friedman, T.B., Riazuddin, S. and Wilcox, E.R. (2001) Mutations of the protocadherin gene *PCDH15* cause Usher syndrome type 1F. *Am. J. Hum. Genet.*, **69**, 25–34.
10. Alagramam, K.N., Yuan, H., Kuehn, M.H., Murcia, C.L., Wayne, S., Srisailpathy, R., Lowry, R.B., Knaus, R., Van Laer, L., Bernier, F.P. *et al.* (2001) Mutations in the novel protocadherin PCDH15 cause Usher syndrome type 1F. *Hum. Mol. Genet.*, **10**, 1709–1718.
11. Gibson, F., Walsh, J., Mburu, P., Varela, A., Brown, K.A., Antonio, M., Beisel, K.W., Steel, K.P. and Brown, S.D.M. (1995) A type VII myosin encoded by the mouse deafness gene *Shaker-1*. *Nature*, **374**, 62–64.
12. Di Palma, F., Holme, R.H., Bryda, E.C., Belyantseva, I.A., Pellegrino, R., Kachar, B., Steel, K.P. and Noben-Trauth, K. (2001) Mutations in Cdh23, encoding a new type of cadherin, cause stereocilia disorganization in waltzer, the mouse model for Usher syndrome type 1D. *Nat Genet.*, **27**, 103–107.
13. Alagramam, K.N., Murcia, C.L., Kwon, H.Y., Pawlowski, K.S., Wright, C.G. and Woychik, R.P. (2001) The mouse Ames waltzer hearing-loss mutant is caused by mutation of Pcdh15, a novel protocadherin gene. *Nat. Genet.*, **27**, 99–102.
14. Self, T., Mahony, M., Fleming, J., Walsh, J., Brown, S.D. and Steel, K.P. (1998) Shaker-1 mutations reveal roles for myosin VIIA in both development and function of cochlear hair cells. *Development*, **125**, 557–566.
15. Boëda, B., El-Amraoui, A., Bahloul, A., Goodyear, R., Daviet, L., Blanchard, S., Perfettini, I., Fath, K.R., Shorte, S., Reiners, J. *et al.* (2002) Myosin VIIa, harmonin and cadherin 23, three Usher I gene products that cooperate to shape the sensory hair cell bundle. *EMBO J.*, **21**, 6689–6699.
16. Kikkawa, Y., Shitara, H., Wakana, S., Kohara, Y., Takada, T., Okamoto, M., Taya, C., Kamiya, K., Yoshikawa, Y., Tokano, H., Kitamura, K., Shimizu, K., Wakabayashi, Y., Shiroishi, T., Kominami, R. and Yonekawa, H. (2003) Mutations in a new scaffold protein *Sans* cause deafness in Jackson shaker mice. *Hum. Mol. Genet.*, **12**, 453–461.
17. Roderick, T.H. (1972) Position of Jackson shaker. *Mouse News Lett.*, **47**, 37.
18. Sedgwick, S.G. and Smerdon, S.J. (1999) The ankyrin repeat: a diversity of interactions on a common structural framework. *Trends Biochem. Sci.*, **24**, 311–316.
19. Ponting, C.P. (1995) SAM: a novel motif in yeast sterile and *Drosophila* polyhomeotic proteins. *Protein Sci.*, **4**, 1928–1930.
20. Schultz, J., Ponting, C.P., Hofmann, K. and Bork, P. (1997) SAM as a protein interaction domain involved in developmental regulation. *Protein Sci.*, **6**, 249–253.
21. Stapleton, C., Balan, I., Pawson, T. and Sicheri, F. (1999) The crystal structure of an Eph receptor SAM domain reveals a mechanism for modular dimerization. *Nat. Struct. Biol.*, **6**, 44–49.
22. Morell, R.J., Friderici, K.H., Wei, S., Elfenbein, J.L., Friedman, T.B. and Fisher, R.A. (2000) A new locus for late-onset, progressive, hereditary hearing loss DFNA20 maps to 17q25. *Genomics*, **63**, 1–6.
23. Yang, T. and Smith, R. (2000) A novel locus DFNA26 maps to chromosome 17q25 in two unrelated families with progressive autosomal dominant hearing loss. *Am. J. Hum. Genet.*, **67**, 300.
24. Sheng, M. and Sala, C. (2001) PDZ domains and the organization of supramolecular complexes. *A. Rev. Neurosci.*, **24**, 1–29.
25. Siemens, J., Kazmierczak, P., Reynolds, A., Sticker, M., Littlewood-Evans, A. and Muller, U. (2002) The Usher syndrome proteins cadherin 23 and harmonin form a complex by means of PDZ-domain interactions. *Proc. Natl Acad. Sci. USA*, **99**, 14946–14951.
26. Kitamura, K., Kakoi, H., Yoshikawa, Y. and Ochikubo, F. (1992) Ultrastructural findings in the inner ear of Jackson shaker mice. *Acta Otolaryngol. (Stockh.)*, **112**, 622–627.
27. Lathrop, G.M., Lalouel, J.M., Julier, C. and Ott, J. (1985) Multilocus linkage analysis in humans: detection of linkage and estimation of recombination. *Am. J. Hum. Genet.*, **37**, 482–498.
28. Küssel-Andermann, P., El-Amraoui, A., Safieddine, S., Nouaille, S., Perfettini, I., Lecuit, M., Cossart, P., Wolfrum, U. and Petit, C. (2000) Vezatin, a novel transmembrane protein, bridges myosin VIIA to the cadherin/catenins complex. *EMBO J.*, **19**, 6020–6029.

Downloaded from https://academic.oup.com/hmg/article/12/5/463/707029 by guest on 20 April 2024